Charge order in β^{″}-phase BEDT-TTF salts

A. Pustogow, K. Treptow, A. Rohwer, Y. Saito, M. Sanz Alonso, A. Löhle, J. A. Schlueter, and M. Dressel

Phys. Rev. B **99**, 155144 — Published 23 April 2019

DOI: 10.1103/PhysRevB.99.155144

Charge Order in β''-phase BEDT-TTF Salts

A. Pustogow,[1] K. Treptow,[1] A. Rohwer,[1] Y. Saito,[1, 2] M. Sanz Alonso,[1] A. Löhle,[1] J. A. Schlueter,[3, 4] and M. Dressel[1]
[1] *1. Physikalisches Institut, Universität Stuttgart, 70569 Stuttgart, Germany*
[2] *Department of Physics, Graduate School of Science, Hokkaido University, Sapporo 060-0810, Japan*
[3] *Material Science Division, Argonne National Laboratory, Argonne, Illinois 60439-4831, U.S.A.*
[4] *Division of Materials Research, National Science Foundation, Alexandria, Virginia 22314, U.S.A.*

(Dated: March 18, 2019)

Experimentally we establish the quantitative phase diagram of 1/4-filled β''-(BEDT-TTF)$_2$SF$_5$*R*SO$_3$ with a tendency towards charge order. Comprehensive optical, transport and susceptibility measurements reveal the insulating nature and magnetic properties of the charge-ordered ground state. Going from $R =$CHF via CH$_2$CF$_2$ and CHFCF$_2$ towards CH$_2$, a finite charge disproportionation appears and grows up to $2\delta = 0.5e$, as evidenced by charge-sensitive molecular vibrations. This is accompanied by an increase of electronic correlation strength, i.e. the inter-site Coulomb repulsion V becomes more pronounced in relation to the bandwidth W. The broadband electronic excitations and their anisotropy unveil a distinct charge pattern for $R =$CH$_2$ (checkerboard-type) as compared to the other compounds (stripe-like). Our results validate theoretical predictions for 1/4-filled systems, substantiating the importance of charge fluctuations for unconventional superconductivity at the verge between metal and insulator.

PACS numbers: 74.70.Kn, 71.30.+h, 75.25.Dk, 74.25.Gz

I. INTRODUCTION

Partial filling of electronic bands commonly features metallic charge transport and is well-described by the tight-binding model[1,2]. For sufficiently small bandwidth, however, the mutual interaction among the conduction electrons triggers localization of charge carriers. While a Mott insulator at 1/2 filling is governed by the on-site term U in relation to the bandwidth W, in 1/4-filled systems the inter-site Coulomb repulsion V gives rise to a charge-ordered ground state described in terms of the extended Hubbard model[3]. In both cases, superconductivity is found at the verge of metal and insulator[4], indicating that Cooper pairing is mediated by the associated low-energy excitations. While in many correlated systems, such as heavy-fermion compounds[5], iron pnictides[6] and high-T_c cuprates[7], spin fluctuations are considered as the driving mechanism, dynamical mean-field theory suggested that also pure charge fluctuations may stabilize unconventional superconductivity[8]. Since both scenarios seem possible, or even intertwined, at 1/2 filling – latest results revealed the importance of metallic quantum fluctuations in the genuine Mott state near the Mott metal-insulator transition[9,10] – it is difficult to separate the individual contributions of charge and spin. On the other hand, magnetic interactions are irrelevant in charge-ordered systems, where the itinerant exchange mechanism is quenched in case of a 1010 charge distribution. Hence, 1/4-filled materials are ideally suited to study pure charge fluctuations as the lowest energy excitations, and their effect on superconductivity. Very recently, we could establish the coexistence of charge order (CO) and superconductivity in β''-(BEDT-TTF)$_2$-SF$_5$CH$_2$CF$_2$SO$_3$[11].

In this work we investigate 1/4-filled organic charge-transfer salts of the (BEDT-TTF)$_2X$ family with quasi two-dimensional electronic properties by means of optical spectroscopy, dc transport and magnetic susceptibility (SQUID) measurements. Upon analyzing the optical properties of β''-(BEDT-TTF)$_2$SF$_5$CH$_2$SO$_3$ (referred to as β''-I) and β''-(BEDT-TTF)$_2$SF$_5$CHFCF$_2$SO$_3$ (β''-MI), and comparing them with the results of β''-(BEDT-TTF)$_2$SF$_5$CH$_2$CF$_2$SO$_3$ (β''-SC) and β''-(BEDT-TTF)$_2$-SF$_5$CHFSO$_3$ (β''-M)[12–14], a generalized phase diagram of the β''-(BEDT-TTF)$_2$SF$_5$*R*SO$_3$ series is established based on electronic correlations V/W as suggested by Girlando *et al.*[14]. While Kaiser *et al.* have studied the effect of charge fluctuations on superconductivity[13], we focus more on the static charge disproportionation leading to insulating ground states. We find that both the charge disproportionation 2δ and transition temperature T_{CO} scale with inter-site Coulomb repulsion V.

II. MATERIALS AND CHARACTERIZATION

β''-(BEDT-TTF)$_2$SF$_5$CH$_2$SO$_3$ and β''-(BEDT-TTF)$_2$SF$_5$CHFCF$_2$SO$_3$ single crystals with dimensions up to $2 \times 2 \times 0.5$ mm^3 were grown by electrochemical methods[15]. The optical reflectivity was measured from as-grown surfaces for polarization along the three main crystal axes in temperature and spectral ranges of 5–295 K and 20–8000 cm^{-1}, respectively. The dc resistivity was acquired in four-point geometry from room temperature down to helium temperatures. Using a commercial superconducting quantum interference device (SQUID), the magnetization at a magnetic field of 0.1 T was recorded as a function of temperature .

Fig. 1 illustrates the anion structure (see Fig. 4(a,b) for the complete crystal structure) and the corresponding positions in the phase diagram of 1/4-filled materials subject to strong electronic interactions[8,12–16]. Table I

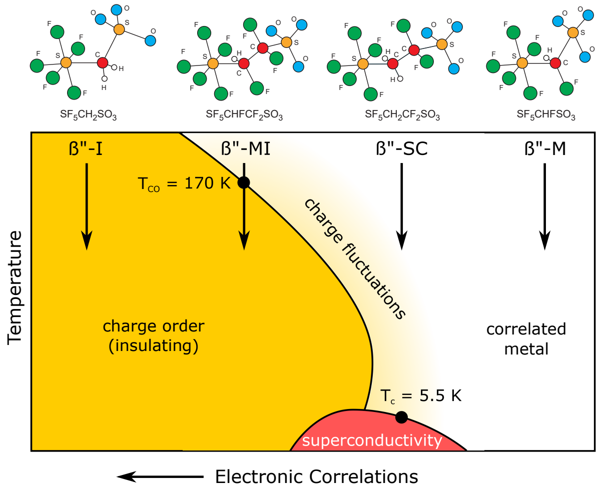

FIG. 1. The anions X of the β''-(BEDT-TTF)$_2$SF$_5R$SO$_3$ series are placed at the tentative position in the phase diagram of 1/4-filled Mott-Hubbard systems. Previous experimental and theoretical investigations[12–16] suggest decreasing correlation strength in the order R = CH$_2$ (β''-I) – CH$_2$ (β''-MI) – CH$_2$ (β''-SC) – CH$_2$ (β''-M).

lists the basic transport and structural characteristics of the β''-(BEDT-TTF)$_2$SF$_5R$SO$_3$ series. β''-I is known to remain insulating up to room temperature, while β''-MI undergoes a metal-insulator transition at 170 K[15]. β''-M and β''-SC are metallic at all temperatures; with β''-SC showing pronounced charge fluctuations and eventually entering the superconducting state[13].

The unit-cell volumes V_{UC} are rather different due to the distinct length of alkyl groups R (cf. Fig. 1): since CH$_2$ and CHF are only about half the size of CHFCF$_2$ and CH$_2$CF$_2$, V_{UC} is significantly smaller for the former two salts. Within each pair of compounds of similarly sized anions, the charge disproportionation 2δ determined according to the Guionneau-Day equation[17] gets smaller as the unit-cell volume increases. The trend of 2δ, however, does not simply follow the order suggested by Girlando *et al.*[14] illustrated in the phase diagram of Fig. 1. This may be explained by the inaccuracy of the Guionneau-Day method[15]. Note, the inter-layer separation $d_\perp$ is significantly shorter for the two metallic systems. Hence, the wave function overlap between the planes is smaller for β''-I and β''-MI, which pronounces the two-dimensionality and nominally reduces the bandwidth; as a result correlations V/W are – as we will later see – stronger for the insulating compounds. On the other hand, the anions are not located between the individual BEDT-TTF molecules, but directly above and below them (cf. Fig. 4a,b); correspondingly the anion-BEDT-TTF separation is reduced.

TABLE I. Metal-insulator transition temperature T_{CO} for the β''-(BEDT-TTF)$_2$SF$_5R$SO$_3$ compounds with a charge-ordered ground state; T_c denotes a superconducting transition temperature. The unit cell volume V_{UC} and inter-layer separation $d_\perp$ (at T = 300 K), as well as the charge disproportionation 2δ determined from the atomic distances within the BEDT-TTF molecule[17] do not exhibit a monotonous trend[15,16].

	β''-I	β''-MI	β''-SC	β''-M
R	CH$_2$	CHFCF$_2$	CH$_2$CF$_2$	CHF
T_{CO} (K)	> 300	170	-	-
T_c (K)	-	-	5.5	-
V_{UC} (Å^3)	1742.45	1841.9	1835.5	1761.55
$d_\perp$ (Å)	17.30	17.35	17.11	17.18
2δ (e)	0.2	0.10	0.14	0.06

As a first characterization, we discuss the transport and magnetic properties of the β''-(BEDT-TTF)$_2$-SF$_5R$SO$_3$ family. Fig. 2(a) displays the temperature dependence of the dc resistivity on a semi-logarithmic scale; the data of β''-SC and β''-M are taken from Ref. 13. The behaviors of β''-I and β''-MI agree well with previous reports[15] in the range T > 77 K. β''-I is first insulating when cooled down with no obvious transition; in the range 100–200 K we extract a transport gap Δ of approximately 10^3 K (Fig. 2c). Below T = 70 K a more metallic behavior is observed with some hysteresis between heating and cooling runs indicating possible structural modifications. β''-MI shows metallic proper-

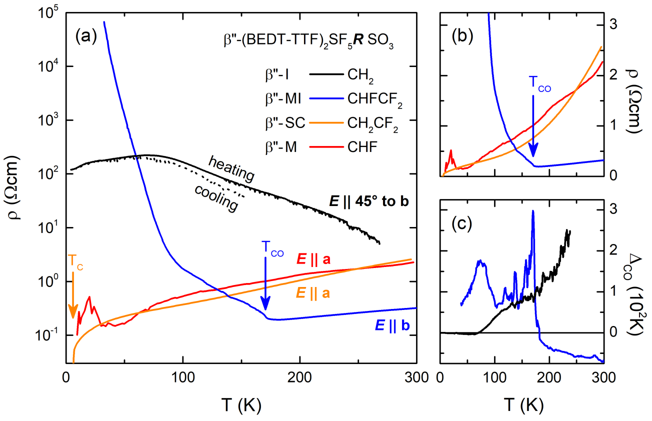

FIG. 2. (a,b) In-plane dc resistivity of β''-(BEDT-TTF)$_2$-SF$_5R$SO$_3$ as a function of temperature. β''-I shows an insulating behaviour at high temperatures, in accord with Ref. 15; below 70 K the resistance decreases towards T = 0. Cooling through the charge-order transition T_{CO} = 170 K the metallic behavior of β''-MI changes to an insulating one; but only below 90 K a strong increase of $\rho(T)$ is observed. β''-SC and β''-M show metallic properties; the former compound becomes superconducting below T_c = 5.5 K (data taken from Ref. 13). (c) The transport gap Δ_{CO} extracted from the Arrhenius plot is of the order of 10^3 K for both β''-I and β''-MI, but with distinct temperature dependence. Note the measurement directions along different crystal axes, yielding distinct absolute values of the resistivity.[18]

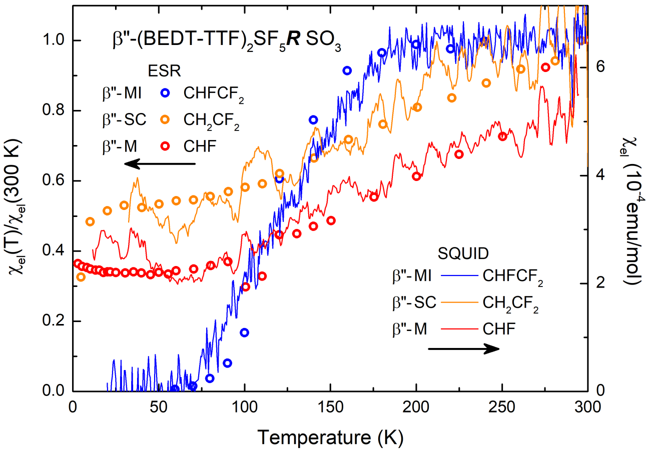

FIG. 3. The spin susceptibility of β''-MI, β''-SC and β''-M was measured by SQUID magnetometry at a field of 0.1 T. A constant was added to account for the diamagnetic background χ_D. The SQUID data (right scale) match well with the electron-spin resonance (ESR) data from Refs. 15, and 19 (left scale). β''-MI shows a pronounced drop of spin susceptibility when charge order sets in below $T_{\rm CO} = 170$ K. χ_{el} basically vanishes at low temperatures indicating spin pairing in the insulating state. The other two compounds remain metallic down to lowest temperatures and show a non-vanishing spin susceptibility arising from Pauli paramagnetism. χ_{el} decreases continuously upon cooling.

ties above $T_{\rm CO} = 170$ K; at lower temperatures it becomes insulating with a pronounced enhancement of the resistivity below 90 K[18].

In addition to electronic transport, we measured the magnetic susceptibility in a SQUID magnetometer at $B = 0.1$ T. Fig. 3 compares $\chi_{el}(T)$ (after subtraction of the constant diamagnetic contribution) for β''-MI, β''-SC and β''-M with the spin susceptibility obtained by electron spin resonance experiments[15,19], the latter being normalized to room temperature. The magnetic field direction was chosen approximately perpendicular to the conducting layers with an accuracy ±15°. In the normal state, the spin susceptibility is positive due to Pauli paramagnetism. The two metallic compounds show a smooth decrease of $\chi_{el}(T)$ by a factor 2 from $T = 300$ K down to low temperatures; it remains more or less constant below 50 K[15,19] indicative of a correlated metallic state.

The spin susceptibility of β''-MI is constant above $T_{\rm CO} = 170$ K reflecting the metallic properties seen in the transport data. In the charge-ordered state, however, $\chi_{el}(T)$ drops significantly until it has basically vanished below 80 K, which coincides with the enhanced increase of resistivity. Considering a stripe-like arrangement of charge-poor and -rich molecules along the crystallographic a-direction[15], we suggest that an antiferromagnetic spin arrangement sets in below $T_{\rm CO}$ due to increased exchange interaction along the stacks.

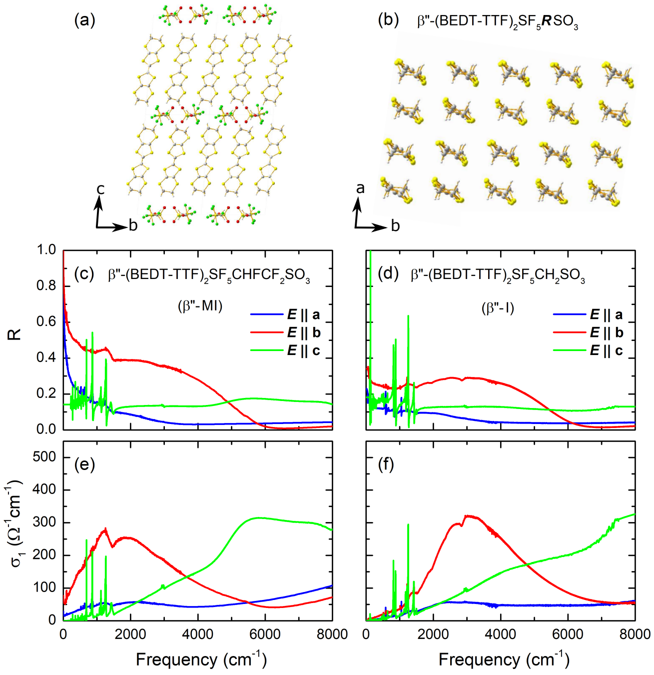

FIG. 4. (a) Crystal structure of β''-(BEDT-TTF)$_2$SF$_5R$SO$_3$ with all-organic anions (here R = CH$_2$CF$_2$) separating the conducting planes. (b) The characteristic β''-arrangement within the BEDT-TTF layers yields stacks along the a-direction; the largest transfer integrals are perpendicular to them, close to the b-axis. Accordingly, the main low-energy absorption is found for $E \parallel b$ in the optical reflectivity and conductivity of β''-MI (c,e) and β''-I (d,f), both of which show very similar properties and anisotropy as the metallic sibling compounds β''-SC and β''-M[13].

III. RESULTS

The focus of our study are broadband in- and out-of-plane optical experiments on β''-I and β''-MI in order to determine the charge disproportionation and pattern, as well as the strength of electronic interactions. The strongly anisotropic optical response of these materials is illustrated in Fig. 4, where the room-temperature reflectivity and the corresponding conductivity are plotted for all three optical axes, which are indicated in the crystal structure of panels (a,b). The overall spectra of both compounds are rather similar to β''-SC and β''-M[12,13]. The conductivity is largest along the crystallographic b-direction with a plasma edge around 6000–7000 cm^{-1}. For the second in-plane polarization ($E \parallel a$) the optical response is also metallic but the plasma frequency significantly lower, $\omega_p \approx 3000$–4000 cm^{-1}.[20] Perpendicular to the conducting planes ($E \parallel c$) the insulating behavior leads to a flat overall reflectivity; the optical conductivity below 2000 cm^{-1} is dominated by numerous sharp molecular vibration modes.

A. Charge Order Revealed by Molecular Vibrations

For determining the molecular charge locally, vibrational spectroscopy has been established as the superior method in the field of organic charge-transfer salts[14,21,22]. In particular we investigate the fully-symmetric charge-sensitive $\nu_{27}(\mathrm{b}_{1u})$ vibration of the BEDT-TTF molecule around 1400–1500cm^{-1} that is best detected for light polarized out-of-plane. In Fig. 5(a) the optical conductivity of the fully insulating compound β''-I is plotted over a broad range; the particular spectral range of the ν_{27} mode is enlarged in panel (b). Already at room temperature two peaks are identified corresponding to inequivalent BEDT-TTF site charges. The frequency separation is slightly reduced upon cooling with $2\delta = 0.47e$ at $T = 5$ K. Most important, however, is the additional splitting that occurs below 100 K; at these temperatures another, minor mode appears around 1466 cm^{-1}. According to Ref. 14, this represents a pretty small amount of BEDT-TTF$^{+0.5}$, and we relate this feature to the onset of metallicity below 100 K, as presented in Fig. 2; the weak intensity implies a negligibly small fraction of normally charged BEDT-TTF. This observation is strongly affirmed by the additional splitting of the peaks at 1430 and 1495 cm^{-1} that occurs at low temperatures. We conclude a small, but noticeable reorganization of charge leading to a superstructure, likely a doubling of the unit cell. The general charge pattern, however, should resemble the high-temperature situation, i.e. the sites remain in their original charge-poor/-rich state with a slight modification $\pm\Delta\rho$ causing a shift on the order of 2 cm^{-1}.

Although the mode $\nu_{27}(\mathrm{b}_{1u})$ provides the most accurate estimate of the molecular charge by infrared spectroscopy due to its close-to-linear frequency-charge relation to the BEDT-TTF site charge[21], we concomitantly inspected several features in the far-infrared range that also prove the distinct ionicities of BEDT-TTF molecules in β''-I. The vibration around 500–530 cm^{-1} plotted in Fig. 6 is assigned to the $\nu_{34}(\mathrm{b}_{1u})$ mode and shows a very similar structure as the ν_{27} vibration. The two main peaks are separated by approximately 15 cm^{-1}; based on the frequencies of neutral BEDT-TTF and its monovalent cation listed in Ref. 14 (there denoted as ν_{31}), the corresponding charge disproportionation at $T = 5$ K is estimated to $2\delta = 0.78e$. We note that possible nonlinearities of $\nu_{34}(\rho)$ may result in an overestimation of 2δ in β''-I.

For comparison, in Fig. 5(c,d) the out-of-plane ($E \parallel c$) response of β''-MI is presented, which exhibits a phase transition around 170 K. The metal-insulator transition is nicely revealed in the temperature dependence of the ν_{27} vibration, where two distinct peaks at 1445 and 1486 cm^{-1} evolve below T_{CO}; they can be identified up to room temperature, but become sharp only when the charges are localized in the insulating state. The splitting of 41 cm^{-1} at $T = 5$ K corresponds to $2\delta = 0.29e$.

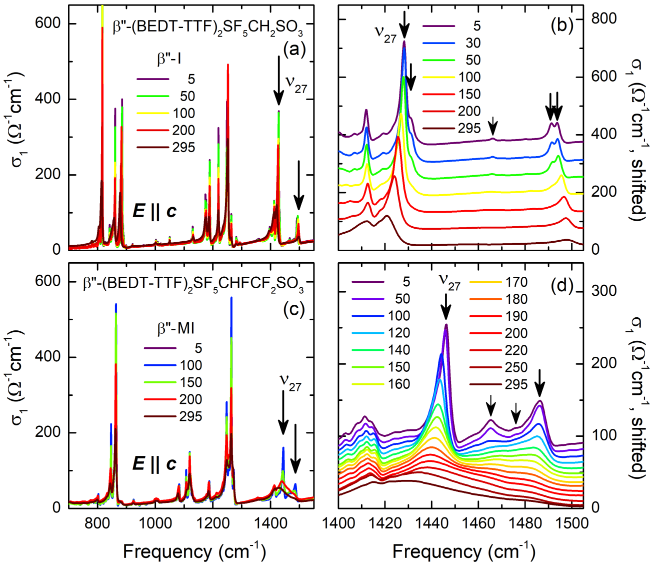

FIG. 5. The out-of-plane ($E \parallel c$) optical conductivity of β''-I (a) and β''-MI (c) is dominated by molecular vibrations on a negligibly small electronic background. The temperature evolution is illustrated by selected temperature values. (b) The charge-sensitive $\nu_{27}(\mathrm{b}_{1u})$ mode of β''-I shows two main peaks at 1428 and 1495 cm^{-1} and a weak satellite at 1467 cm^{-1}. The splitting corresponds to a charge disproportionation of $2\delta = 0.46e$ at $T = 5$ K. While the peak separation does not change much with temperature, the main features split up into doublets below 100 K, as illustrated by the arrows. (d) For β''-MI there are two main peaks at 1445 and 1486 cm^{-1}, corresponding to $2\delta = 0.29e$ at 5 K, which are already present at room temperature. They narrow significantly in the charge-ordered state below $T_{\mathrm{CO}} = 180$ K. When cooled below 120 K, the satellite around 1470 cm^{-1} splits into two peaks. The modes around 1410 cm^{-1} correspond to ethylene end group vibrations involving hydrogen atoms. The data in (b) and (d) are vertically offset for clarity reasons.

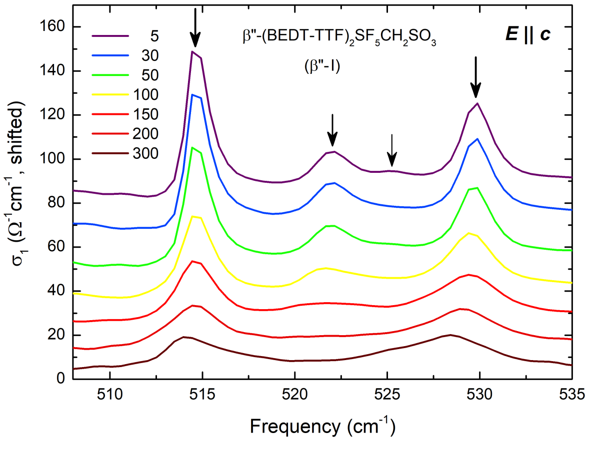

FIG. 6. In the far-infrared spectral range, the insulating salt β''-I reveals the charge-sensitive $\nu_{34}(\mathrm{b}_{1u})$ mode, which exhibits a structure very similar to the ν_{27} mode. The separation of the two main peaks is approximately 15 cm^{-1} corresponding to a charge disproportionation of $2\delta = 0.78e$ at low temperatures. The data are vertically shifted with respect to each other.

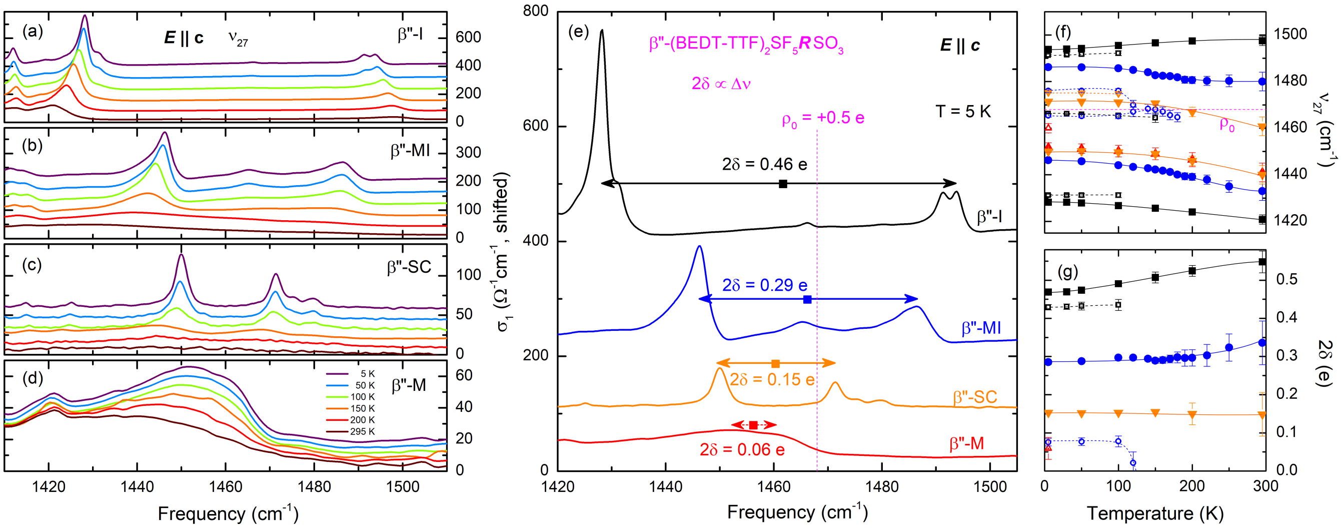

FIG. 7. Temperature evolution of the charge-sensitive mode $\nu_{27}(\mathrm{b}_{1u})$ compared (a) for the insulating salt β''-I, (b) for β''-MI, (c) for the superconductor β''-SC and (d) for the all-metallic compound β''-M. The data for the latter two compounds are reproduced from Ref. 12. While β''-M shows only one sizeable feature (possibly consisting of two broad modes very close to each other) at all temperatures, the modes of the other compounds significantly narrow and split when the temperature decreases. (e) The modes are compared on a common scale for the lowest temperature, with the solid squares indicating the average peak position $(\nu_{\max}+\nu_{\min})/2$; the vertical magenta line indicates the position of the BEDT-TTF$^{+0.5}$ molecule reported in the literature[14,22]. In the case of β''-M we give only an upper bound of the peak separation. Apparently, the features become narrower and more intense as the charge disproportionation is enhanced. The data are vertically shifted. (f) Temperature dependence of the ν_{27} resonance frequencies determined by fitting the modes in panels (a-d). One can nicely see that the peaks split more or less symmetrically around the $0.5e$ position located at 1460 - 1470 cm^{-1}. While initially most of the modes show blue-shifts upon cooling, the general structure remains basically constant below T = 100 K. The small open symbols denote satellite peaks. (g) Molecular charge separation $2\delta(T)$ as a function of temperature; the amount of charge disproportionation is significantly reduced among the compounds in the order β''-I – β''-MI – β''-SC – β''-M. We ascribe this to decreasing inter-site Coulomb repulsion and correlation effects in the β''-(BEDT-TTF)$_2$SF$_5R$SO$_3$ series. Solid, dashed lines are guides to the eye.

Two minor features appear at low temperatures, located around the frequency of BEDT-TTF$^{+0.5}$, where the one at 1465 cm^{-1} bears significantly more spectral weight than the intermediate peak in β''-I discussed with respect to Fig. 5 (b). Since β''-MI is strongly insulating at low temperatures, it becomes clear that the bare occurrence of a BEDT-TTF$^{+0.5}$ mode does not allow us to conclude on a metallic behavior. Therefore, we do not consider these intermediate features with small intensity in the following. Note that the vibrations around 1410 cm^{-1} are related to the ethylene endgroups – the involvement of hydrogen atoms was evidenced by comparing the out-of-plane infrared spectra of β''-SC and its deuterated analogue[11]. The assignment is confirmed by the fact that this feature at 1410 cm^{-1} does not change position; in contrast to the ν_{27} mode, which exhibits pronounced shifts between the different compounds as well as upon cooling.

Observing significant differences of ionicity between the molecular sites constitutes direct evidence for the charge-ordered nature of the insulating state in β''-I and in β''-MI. In Fig. 7 the temperature-dependent ν_{27} spectra of all four β''-(BEDT-TTF)$_2$SF$_5R$SO$_3$ compounds are summarized, including previously obtained results[12]. In all cases, the vibrational features get more pronounced and sharpen as the temperature is reduced, as reproduced in panels (a-d). Hence we focus on the 5 K spectra and combine them in Fig. 7(e) for comparison. The charge disproportionation continuously decreases when going from the insulating β''-I ($2\delta = 0.46e$ for T = 5 K) via β''-MI ($2\delta = 0.29e$) and β''-SC ($2\delta = 0.15e$) to the metallic compound β''-M ($2\delta < 0.06e$ at the lowest temperature). Following the suggestion of Girlando *et al.*[14], this order corresponds to the strength of effective inter-site correlations, summarized in the phase diagram (cf. Fig.1). A similar relation between 2δ and the strength of electronic correlations V/W was reported for the charge-ordered phase in the quasi one-dimensional Fabre salts (TMTTF)$_2X$ [23,24]. In general, the intensity of the individual modes increases with hole density, i.e. towards lower frequencies; these observations are in excellent agreement with quantum chemical calculations[14]. As the charge imbalance 2δ becomes smaller when going from β''-I to β''-M, we observe a significant broadening of the vibrational peaks. This reflects the close link between the amount of redistributed charge and the charge localization and fluctuation strength. It was proposed[14] that fluctuating (broad modes) and localized (separated sharp peaks) charges coexist in β''-SC; conversely, the absence of broad features in the low-temperature ν_{27} spectra of the insulating β''-I and β''-MI compounds is fully in line with these arguments.

For a quantitative comparison, the ν_{27} resonance frequencies and the corresponding charge disproportionation are plotted in Fig. 7(f,g) as a function of temperature. For β''-I and β''-MI the two main peaks are split more or less symmetrically around the BEDT-TTF$^{+0.5}$ position at 1468 cm^{-1}. For completeness reasons, also the minor features are plotted as small, empty symbols. In Fig. 7(g) we can see that in all four β''-(BEDT-TTF)$_2$-SF$_5$$RSO_3$ compounds the temperature dependence of 2δ is rather weak. The intensity of the vibrational features strongly increases upon cooling, but the charge disproportionation remains basically unaffected, it might even decrease for the insulating compounds.

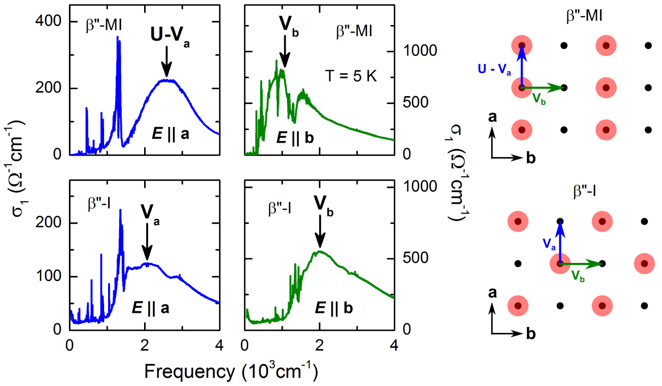

FIG. 8. Different charge patterns in β''-MI and β''-I as inferred from optical spectroscopy results. While for β''-MI the charge-poor and -rich molecules arrange in stripes along the a-axis, in β''-I a checkerboard pattern is observed. In the latter case, excitations along both in-plane axes occur between charge-poor and -rich molecules and cost the energy V_a and V_b, which are almost identical. In β''-MI such excitations appear only for $E \parallel b$ whereas transitions between charge-rich sites along the a-axis create double occupancies with an additional on-site penalty U, shifting the Mott-Hubbard band to higher energy.

B. Broadband Response: Electronic Excitations and Charge Pattern

Now we turn to the in-plane electrodynamic response of β''-(BEDT-TTF)$_2$SF$_5$$RSO_3$, which yields valuable information on the interaction strength and correlations. The optical conductivity maps the electronic transitions between the Hubbard bands; thus the shape of $\sigma_1(\omega)$ reflects the band structure. If we assume a single-band, 1/2-filled Mott insulator, the lower and upper Hubbard bands both will have the bandwidth W and will be shifted by U[25,26]. The electronic excitations are symmetric and produce a broad absorption feature in the optical properties centered at U with a width of $2W$[9]. On the other hand, 3/4-filled systems are prone to charge order when the inter-site Coulomb repulsion V is sufficiently strong. The upper Hubbard band consists of unoccupied states with a weight of 1/4 of the original band and the lower Hubbard band constitutes 3/4 of the electronic states; hence the corresponding transitions are not symmetric, at least on the high-energy wing of the band.

In Fig. 8 we contrast the low-temperature spectra of β''-I and β''-MI for both polarizations and sketch the respective charge pattern with the corresponding transitions. We associate the distinct optical excitations with specific charge arrangements in the two materials. In the former compound, we see the charge-rich A ($\rho = 0.5 + \delta$) and charge-poor B ($0.5 - \delta$) sites arranged along $-a + b$, i.e. diagonal direction, in accord with Ref. 15. For the other three β''-(BEDT-TTF)$_2$SF$_5$$RSO_3$ compounds, including β''-MI shown here, the stripes form parallel to the a-axis.

The checkerboard arrangement observed for β''-I implies that the charge-poor and -rich molecules alternate along both the a- and b-axes. Hence, nearest-neighbor excitations always move a charge from an occupied to an empty site which incurs an additional inter-site Coulomb energy V[27]. The situation is different for the stripe-like pattern found in β''-MI, which – in the limit of $2\delta = 1e$ – would correspond to alternating one-dimensional arrays of completely occupied and empty sites, the former of which constitute effectively 1/2-filled chains while the latter are unoccupied. Thus, transitions for $E \parallel a$ can be treated like for 1/2-filled Mott insulators. As the charge is excited among charge-rich molecules, the inter-site repulsion V_a is reduced on the expense of the on-site Coulomb energy U due to creation of a double occupancy. Since $U \gg V_i$, the corresponding Mott-Hubbard band peaks at higher frequencies. On the other hand, excitations perpendicular to a ($E \parallel b$) move an electron from a charge-rich to a charge-poor site, reducing the intra-stripe repulsion to the nearest neighbors in $\pm a$ direction at the cost of the inter-stripe repulsion. As a result, the excitation energy V_b is significantly lower because the reduced repulsion along a is of comparable order of magnitude as the increase along b-direction.[27] The stripe pattern suggests an enhanced one-dimensional coupling of the spins on the charge-rich sites, similar to the itinerant exchange mechanism in a 1/2-filled Mott insulator, which may be the reason for the vanishing spin susceptibility below the phase transition in β''-MI, displayed in Fig. 3. As noted before, these considerations apply to the extreme case $2\delta = 1e$; for smaller charge disproportionation each transition involves a finite on-site Coulomb repulsion Un_in_j because $n_i \neq 0$ even on the charge-poor sites. However, such an on-site term does not introduce anisotropy to the checkerboard pattern of β''-I since the amount of charge on the nearest-neighbor sites along a and b is identical. The slight difference in band shapes among the two in-plane polarizations may be related to the splitting of the ν_{27} mode below $T = 100$ K, yielding minor differences for excitations parallel to a as compared to the b-axis.

Fig. 9(a,b) displays the in-plane optical properties of

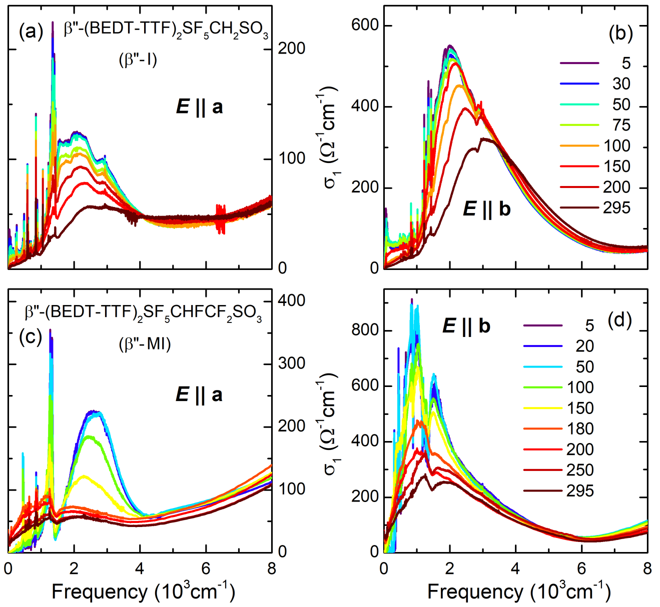

FIG. 9. Broadband optical conductivity of β''-I and β''-MI measured for different temperatures along the two main polarizations, $E \parallel a$ and $E \parallel b$. (a,b) For both directions β''-I exhibits a pronounced Mott-Hubbard band with increasing intensity upon cooling. The strong upturn of conductivity in the far-infrared at low temperatures indicates a narrow Drude contribution. (c,d) The in-plane optical response of β''-MI is strongly anisotropic. For $E \parallel a$ the Mott-Hubbard band is centered between 2000–3000 cm^{-1}. Along the b-direction it peaks around 1000 cm^{-1} and acquires a strongly asymmetric shape.

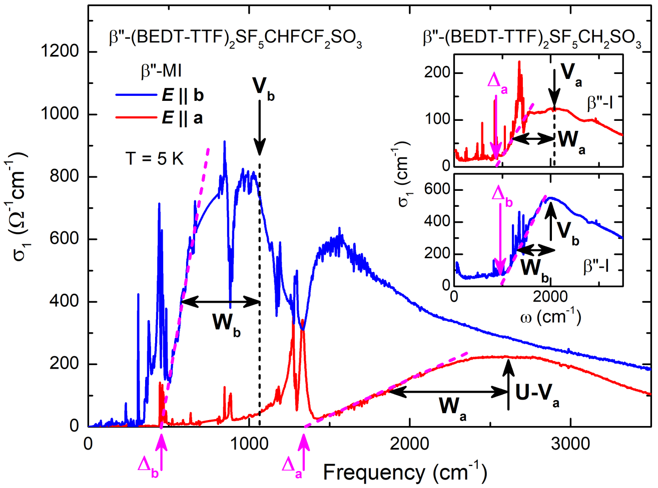

FIG. 10. Low-temperature optical conductivity of β''-MI and β''-I (insets) for the two polarizations within the highly conducting plane, $E \parallel a$ and b. From the maxima of the bands, the respective Coulomb interaction can be extracted, as indicated; see text and Fig. 8 for details. The linear extrapolations of the low-frequency edge are used to determine the Mott-Hubbard gaps Δ_i ($i = a, b$), indicated by the dashed magenta lines. The bandwidth W is estimated at half maximum. At 100 K $\leq T \leq$ 150 K the transport gap size (cf. Fig. 2c) coincides with the low-temperature optical results. Insets: Although shape and intensities of the bands are not identical, the bandwidth, gap size and Coulomb repulsion are similar for the two in-plane polarizations of β''-I, indicating almost isotropic conduction properties.

β''-I recorded at various temperatures. The spectra in the mid-infrared range agree well with previous studies[28]. For both polarizations within the conducting plane, the overall intensity of the Mott-Hubbard band increases upon cooling with an optical gap around 900 cm^{-1} (Fig. 10); this is in fair agreement with the activation energy Δ_{CO} obtained from transport measurements, shown in Fig. 2. In addition, a narrow, weak Drude-like contribution appears below T = 100 K corresponding to the metallic behavior observed by low-temperature transport measurements on the very same specimen.

The situation is different for β''-MI, which exhibits strongly anisotropic electronic properties, as shown in Fig. 9(c,d). In particular for $E \parallel a$, we observe a rapid change in conductivity around 170 K when the material becomes insulating; a pronounced gap opens for both polarizations and the spectral weight shifts to higher energies intensifying the Mott-Hubbard band. The overall gap size and Coulomb repulsion are larger for $E \parallel a$. As seen in the magnified presentation of Fig. 10, in this direction the electronic excitations are centered around 2600 cm^{-1} and the gap is estimated somewhere above 1000 cm^{-1}, with some uncertainty due to the strong vibrational features[29]. While appearing as positive peaks around 1300 cm^{-1} along a, these molecular vibrations show up as pronounced dips for $E \parallel b$ because of strong emv-coupling to the large electronic background in the same frequency range. On the other hand, the Mott-Hubbard transition peaks around 1000 cm^{-1}, and the sharp band edge below 500 cm^{-1} shows good agreement with the transport data. We also determine the bandwidth W as the half-width at half maximum, which is larger for the a-axis. Since the interaction is stronger along this crystallographic direction, however, electronic correlations are less pronounced for $E \parallel b$.

C. Experimental Phase Diagram of Charge Order

Our present investigations combined with previous studies[12–14,28] provide a solid basis for the overall understanding of the microscopic charge arrangement in the β''-phase BEDT-TTF salts. The optical spectra of all β''-(BEDT-TTF)$_2$SF$_5$$RSO_3$ compounds recorded in both in-plane polarizations are summarized in Fig. 11. The overall shape is rather similar and in general the intensity is larger for the polarization $E \parallel b$; this indicates that for all compounds the spectral features have a common origin, namely excitations between charge-poor and charge-rich sites. It is interesting to note that β''-SC exhibits a well-defined Mott-Hubbard band only for $E \parallel b$ –

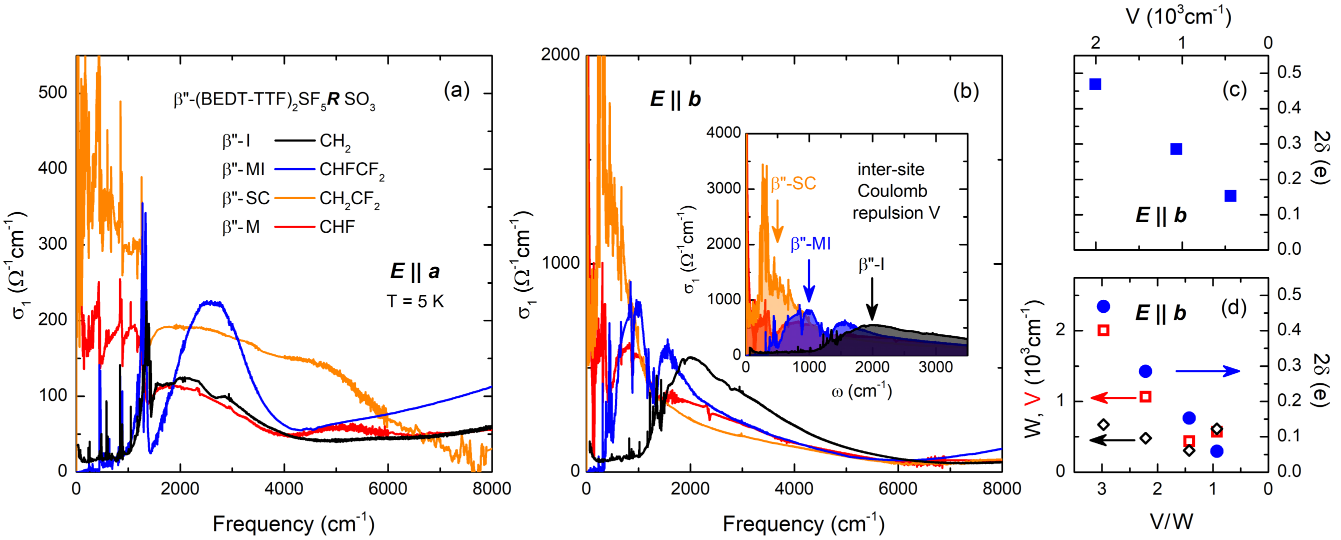

FIG. 11. In-plane optical conductivity of the four β''-(BEDT-TTF)$_2$SF$_5R$SO$_3$ compounds, β''-I, β''-MI, β''-SC, and β''-M, obtained at the lowest temperatures for (a) $E \parallel a$ and (b) $E \parallel b$. The inset points out the excitation energy for transitions between charge-poor and -rich sites; the inter-site Coulomb interaction V decreases in the fashion β''-I – β''-MI – β''-SC. (c,d) The charge disproportionation 2δ increases with V and V/W in accord with the extended Hubbard model (cf. Fig. 1 and Ref. 14). The interaction parameters V, W in (d) were determined according to Fig. 10.

very similar to β''-MI; it occurs at lower frequency, however, in accord with the smaller charge disproportionation 2δ. The transition along the a-direction appears at higher energy and it is much broader in β''-SC than for β''-MI, reflecting the larger bandwidth.

For the direction $E \parallel a$, a quantitative comparison between the materials is not straight forward because the charge patterns are different and there is a rather dominant metallic background for β''-SC and β''-M, which inhibits separation and unambiguous identification of the Mott-Hubbard bands[30]. Along the b-axis, however, the spectral features of all compounds correspond to electronic excitations from charge-poor to charge-rich sites and thus are related to the inter-site Coulomb energy V. As shown in the inset of Fig. 11(b), the interaction strength is largest for β''-I and decreases to β''-MI and β''-SC; within the error bars V is comparable, or slightly larger for β''-M than for β''-SC. By extracting the band parameters V and W from the Mott-Hubbard bands following Fig. 10, we find that the charge disproportionation 2δ follows V and V/W in a monotonous fashion, which is shown in Fig. 11(c,d). This corroborates the main assumption that charge order in these compounds is driven mainly by intersite Coulomb repulsion and can be treated in terms of the extended Hubbard model. The fact that the order parameter 2δ is suppressed with decreasing correlation strength V/W provides conclusive evidence that the underlying physics is satisfactorily described by bandwidth tuning, advancing the phase diagram of charge-ordered systems to a solid framework – similar as for Mott insulators at 1/2-filling[9]. To summarize our endeavour, we assembled a quantitative phase diagram (Fig. 12) based on the experimental findings (2δ, V/W) of this work. We thus provide evidence that the charge-ordered phase truly is the result of inter-site Coulomb interactions and superconductivity emerges right at the verge between metal and insulator, classifying the β''-(BEDT-TTF)$_2$SF$_5R$SO$_3$ series as a paradigmatic correlated electron system at 1/4 filling.

IV. DISCUSSION

The extensive comparison of four different molecular conductors driven by the same physics enables us to investigate the charge-ordering phenomenon in never seen detail. It appears from Fig. 7 (f,g) that the charge disproportionation does not exhibit a pronounced temperature dependence for any member of the β''-(BEDT-TTF)$_2$-SF$_5R$SO$_3$ family – 2δ even remains unchanged as β''-MI crosses $T_{\rm CO}$. This is strikingly different compared to electronic CO in quasi one-dimensional (TMTTF)$_2X$ where the order parameter increases in a second-order, mean-field fashion below $T_{\rm CO}$[23,24,31]. The behavior of β''-(BEDT-TTF)$_2$SF$_5R$SO$_3$ differs also from the paradigmatic charge-order material α-(BEDT-TTF)$_2$I$_3$, where the molecular charge varies abruptly at the metal-insulator transition[32,33] and reveals a clear first-order transition with phase coexistence[34]. Moreover, the absence of temperature dependence of 2δ and its decoupling from the general conduction properties through the phase transition may point to an external origin, for instance like anion ordering in (TMTTF)$_2X$[24].

A close look on the average charge per molecule yields ionicities around $\frac{1}{2}(\rho_{\rm rich} + \rho_{\rm poor}) \approx +0.55e$, slightly larger than $\rho_0 = +0.5e$, but no clear trend is found in

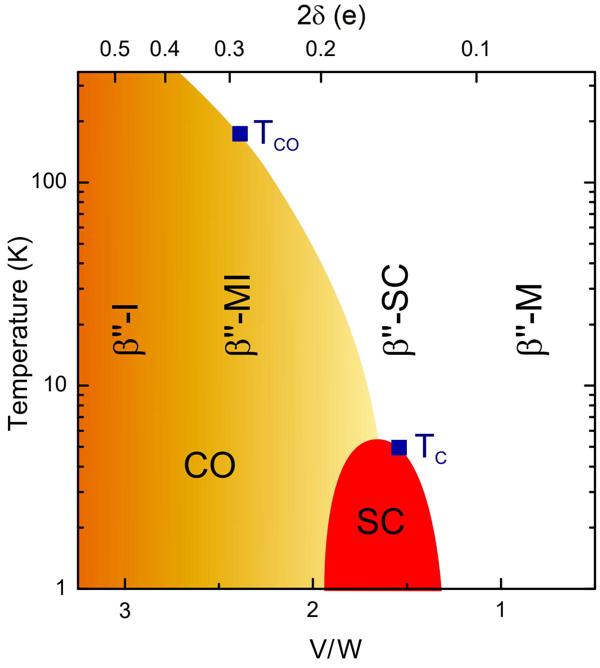

FIG. 12. The results on the charge disproportionation 2δ and the electronic correlation strength V/W (Figs. 7 and 11) are combined to a quantitative phase diagram. The β''-(BEDT-TTF)$_2$SF$_5$$RSO_3$ series thus truly realizes a paradigmatic correlated electron system at 1/4 filling with a superconducting state emerging between metal and insulator[8], validating the suggestions of Girlando and collaborators[14].

relation to 2δ, V and V/W of the four compounds under study. Neglecting β''-I for the moment, which has a different charge pattern, there is a tendency of increasing 'doping' away from ρ_0 as the metallic state is approached in the sequence β''-MI – β''-SC – β''-M. A combined effect of correlations and doping on superconductivity in β''-SC seems possible – a consideration that was already applied towards θ-(BEDT-TTF)$_2$I$_3$[35]. Deviations from 1/4 filling were also suggested by calculations based on the structure, yet towards less positively charged donors $\rho < \rho_0$.[36] We have to stress here, however, that the resonance frequency of the BEDT-TTF ν_{27} mode deviates from +0.5 e in many related materials[37–40], which may be a result of structural properties rather than doping – in particular for the moderate (5–10 cm^{-1}) frequency shifts observed in our case. Further low-temperature studies on the ground state, e.g. by magnetic resonance, Hall effect or dielectric spectroscopy, may elucidate the origin of charge order in the materials studied here, and a possible doping effect.

Let us finally comment on the small, but noticeable reduction of 2δ in β''-I upon cooling that – together with the splitting of the ν_{27} mode – seemingly coincides with the emerging metallicity at low temperatures. Although we also observe enhanced conductivity in our dc transport (Fig. 2) and low-frequency optical (Fig. 9a,b) results, we can only speculate about the origin. One possibility for the drop of resistivity are impurities such as BEDT-TTF$^{+0.5}$ – indeed, there is a minor feature close to the resonance frequency for $\rho_0 = 0.5$ which seems unrelated to the main peaks. A small number of free carriers is in accord with the low plasma frequency and marginal spectral weight of the metallic-like low-energy and dc response. On the other hand, the slow increase of resistivity in β''-I upon cooling may be related to additional doped charge carriers, which undergo a Kondo-like transition below 70 K. Apart from that, the pronounced thermal hysteresis in $\rho(T)$ suggests an involvement of the structural degrees of freedom in the conduction properties. Since the overall electrodynamic response is dominated by the Hubbard bands, however, the relevant physics in β''-I is that of an insulator, legitimating the position of this compound on the strongly correlated side of the phase diagram (Fig. 12). After all, the charge excitations in β''-(BEDT-TTF)$_2$SF$_5$$RSO_3$ provide a clear picture in the sense of Mott-Hubbard physics at 1/4 filling, irrespective of the origin of the repulsive Coulomb interaction that triggers charge order.

It might be worth, to go back to the family of α-(BEDT-TTF)$_2$$M$Hg(SCN)$_4$ salts with M = Tl, Rb, K and NH$_4$, which also exhibit density waves, charge order, and superconductivity[41–45]. Maybe the 1/4-filled compounds can be summarized in a generic phase diagram, similar to the 1/2-filled Mott systems[9].

V. CONCLUSION

Here we could establish the phase diagram of β''-(BEDT-TTF)$_2$SF$_5$$RSO_3$ in accord with previous suggestions[8,14] from our comprehensive dc transport, magnetic and, especially, optical experiments. In particular, we quantitatively evaluate the 1/4-filled compounds on basis of their electronic correlation strength: V/W decreases in the order R = CH$_2$ – CHFCF$_2$ – CH$_2$CF$_2$ – CHF. The two-dimensional nature as well as the metallic and insulating properties of the electronic systems are revealed from the anisotropic electrodynamic response. Employing vibrational spectroscopy, we distinguish different site charges $\rho_0 \pm \delta$ associated with the charge-ordered nature of the insulating states in these materials with effectively 1/4-filled bands. The charge disproportionation 2δ increases with larger Coulomb repulsion V and correlation strength V/W, similar as in the well-understood (TMTTF)$_2$$X$[23,24], providing evidence for Mott-Hubbard physics as the decisive mechanism for electrodynamics. From the polarization-dependent peak position of the broadband infrared absorption, mapping the electronic transitions between lower and upper Hubbard bands, we can directly examine the specific charge pattern within the BEDT-TTF planes. In particular, the electronic excitations are strongly anisotropic for R = CHFCF$_2$ and CH$_2$CF$_2$ implying a stripe-like arrangement of charge-poor and charge-rich molecules along the crystallographic a-direction, in excellent agreement with our SQUID data (cf. Fig. 3) and the structural properties[15]. Therefore, our results confirm that these four materials can be summarized in a common phase diagram in the order β''-I – β''-MI – β''-SC – β''-M for decreasing electronic interactions and charge disproportionation. This consistent picture substantiates the notion that superconductivity in β''-SC is driven by charge fluctuations[8,11,13] as a result of strong electronic correlations.

ACKNOWLEDGMENTS

We appreciate many helpful discussion with S. Brown, H. Jeschke, A. Girlando, J. Merino and J. Wosnitza. The project was supported by the Deutsche Forschungsgemeinschaft (DFG) via DR228/39-1.

---

[1] N. W. Ashcroft and N. D. Mermin, *Solid State Physics* (Harcourt College Publishers, Fort Worth, 1976).

[2] J. Singleton, *Band Structure and Electronic Properties of Solids* (Oxford University Press, Oxford, 2001).

[3] F. Gebhard, *The Mott Metal-Insulator Transition* (Springer-Verlag, Berlin, Heidelberg, 1997).

[4] M. Imada, A. Fujimori, and Y. Tokura, Rev. Mod. Phys. **70**, 1039 (1998).

[5] C. Pfleiderer, Rev. Mod. Phys. **81**, 1551 (2009).

[6] Q. Si, R. Yu, and E. Abrahams, Nature Rev. Mater. **1**, 16017 (2016).

[7] B. Keimer, S. A. Kivelson, M. R. Norman, S. Uchida, and J. Zaanen, Nature **518**, 179 (2015).

[8] J. Merino and R. H. McKenzie, Phys. Rev. Lett. **87**, 237002 (2001).

[9] A. Pustogow, M. Bories, A. Löhle, R. Rösslhuber, E. Zhukova, B. Gorshunov, S. Tomić, J. A. Schlueter, R. Hübner, T. Hiramatsu, Y. Yoshida, G. Saito, R. Kato, T.-H. Lee, V. Dobrosavljević, S. Fratini, and M. Dressel, Nat. Mater. **17**, 773 (2018).

[10] M. Dressel and A. Pustogow, J. Phys. Condens. Matter **30**, 203001 (2018).

[11] A. Pustogow, Y. Saito, A. Rohwer, J. A. Schlueter, and M. Dressel, Phys. Rev. B **XX**, YYYYYY (2019).

[12] N. Drichko, S. Kaiser, Y. Sun, C. Clauss, M. Dressel, H. Mori, J. Schlueter, E. I. Zhyliaeva, S. A. Torunova, and R. N. Lyubovskaya, Physica B: Condens. Matter **404**, 490 (2009).

[13] S. Kaiser, M. Dressel, Y. Sun, A. Greco, J. A. Schlueter, G. L. Gard, and N. Drichko, Phys. Rev. Lett. **105**, 206402 (2010); S. Kaiser, S. Yasin, N. Drichko, M. Dressel, T. Rõõm, D. Hüvonen, U. Nagel, G. L. Gard, and J. A. Schlueter, Phys. Status Solidi B **249**, 985 (2012).

[14] A. Girlando, J. Phys. Chem. C **115**, 19371 (2011); A. Girlando, M. Masino, S. Kaiser, Y. Sun, N. Drichko, M. Dressel, and H. Mori, Phys. Status Solidi B **249**, 953 (2012); A. Girlando, M. Masino, J. A. Schlueter, N. Drichko, S. Kaiser, and M. Dressel, Phys. Rev. B **89**, 174503 (2014).

[15] B. H. Ward, J. A. Schlueter, U. Geiser, H. H. Wang, E. Morales, J. P. Parakka, S. Y. Thomas, J. M. Williams, P. G. Nixon, R. W. Winter, G. L. Gard, H.-J. Koo, and M.-H. Whangbo, Chem. Mater. **12**, 343 (2000); J. A. Schlueter, B. H. Ward, U. Geiser, H. H. Wang, A. M. Kini, J. Parakka, E. Morales, H.-J. Koo, M.-H. Whangbo, R. W. Winter, J. Mohtasham, and G. L. Gard, J. Mater. Chem. **11**, 2008 (2001).

[16] U. Geiser, J. A. Schlueter, H. H. Wang, A. M. Kini, J. M. Williams, P. P. Sche, H. I. Zakowicz, M. L. VanZile, J. D. Dudek, P. G. Nixon, R. W. Winter, G. L. Gard, J. Ren, and M.-H. Whangbo, J. Am. Chem. Soc. **118**, 9996 (1996).

[17] P. Guionneau, C. Kepert, G. Bravic, D. Chasseau, M. Truter, M. Kurmoo, and P. Day, Synth. Met. **86**, 1973 (1997).

[18] Note, that for β''-MI $\rho(T)$ was probed along the crystallographic b-axis where the wave function overlap is largest; hence the absolute value of resistivity in the metallic state, $\rho(T > T_{\mathrm{CO}})$, is almost one order of magnitude lower compared to β''-SC and β''-M, which were measured parallel to the a-axis, i.e. the in-plane direction with the lowest conductivity. For comparison, the deuterated sister compound β''-d$_8$SC has a similar room temperature value $\rho(300K) = 0.2~\Omega\mathrm{cm}$[46,47] along b. The in-plane resistivity of β''-I was measured at 45° with respect to the b-axis. One may speculate that for β''-(BEDT-TTF)$_2$SF$_5R$SO$_3$ the conduction properties are reduced by a smaller anion size. One should keep in mind, however, that for transport measurements a considerable uncertainty occurs in the geometry factor.

[19] H. H. Wang, M. L. VanZile, J. A. Schlueter, U. Geiser, A. M. Kini, P. P. Sche, H.-J. Koo, M.-H. Whangbo, P. G. Nixon, R. W. Winter, and G. L. Gard, J. Phys. Chem. B **103**, 5493 (1999).

[20] Note, for β''-MI the polarization denoted '$E \perp b$' in Ref. 48 corresponds to the crystallographic c-direction rather than the in-plane component $E \parallel a$.

[21] T. Yamamoto, M. Uruichi, K. Yamamoto, K. Yakushi, A. Kawamoto, and H. Taniguchi, J. Phys. Chem. B **109**, 15226 (2005).

[22] M. Dressel and N. Drichko, Chem. Rev. **104**, 5689 (2004).

[23] M. Dressel, M. Dumm, T. Knoblauch, and M. Masino, Crystals **2**, 528 (2012); T. Knoblauch and M. Dressel, Phys. Status Solidi C **9**, 1158 (2012); R. Rösslhuber, E. Rose, T. Ivek, A. Pustogow, T. Breier, M. Geiger, K. Schrem, G. Untereiner, and M. Dressel, Crystals **8**, 121 (2018).

[24] A. Pustogow, T. Peterseim, S. Kolatschek, L. Engel, and M. Dressel, Phys.Rev. B **94**, 195125 (2016).

[25] A. Georges, G. Kotliar, W. Krauth, and M. J. Rozenberg, Rev. Mod. Phys. **68**, 13 (1996); M. J. Rozenberg, G. Kotliar, and H. Kajueter, Phys. Rev. B **54**, 8452 (1996).

[26] J. Merino, M. Dumm, N. Drichko, M. Dressel, and R. H. McKenzie, Phys. Rev. Lett. **100**, 86404 (2008).

[27] Strictly speaking, we have to sum up one inter-site Coulomb repulsion term for each nearest neighbor projected along a and b. In the specific case of β''-I this would be one b-contribution and two a-terms for excitation along b, and *vice versa* for $E \parallel a$. Also next-nearest neighbor terms or higher-order contributions can become relevant, so we define here V_a and V_b as the total sums of inter-site

Coulomb interactions upon moving a charge along a or b, respectively.

[28] I. Olejniczak, B. Barszcz, A. Szutarska, A. Graja, R. Wojciechowski, J. A. Schlueter, A. N. Hata, and B. H. Ward, Phys. Chem. Chem. Phys. **11**, 3910 (2009); I. Olejniczak, B. Barszcz, A. Graja, and J. A. Schlueter, Mater. Sci. Pol. **27**, 619 (2009).

[29] For determination of the optical gap, the steepest slope of the band edge was extrapolated to $\sigma_1 = 0$.

[30] To fit the data in Ref. 13 satisfactorily, several terms were necessary corresponding to the broad features in the far- and mid-infrared ranges. Hence, there remains some ambiguity in determining the peak position of the Mott-Hubbard features in β''-M; nevertheless, within this uncertainty, V is not significantly larger than in β''-SC.

[31] Y. Oka, N. Matsunaga, K. Nomura, A. Kawamoto, K. Yamamoto, and K. Yakushi, J. Phys. Soc. Jpn. **84**, 114709 (2015).

[32] Y. Yue, K. Yamamoto, M. Uruichi, C. Nakano, K. Yakushi, S. Yamada, T. Hiejima, and A. Kawamoto, Phys. Rev. B **82**, 75134 (2010).

[33] T. Ivek, B. Korin-Hamzić, O. Milat, S. Tomić, C. Clauss, N. Drichko, D. Schweitzer, and M. Dressel, Phys. Rev. B **83**, 165128 (2011).

[34] A. Pustogow, A. S. McLeod, Y. Saito, D. N. Basov, and M. Dressel, Sci. Adv. **4**, eaau9123 (2018).

[35] B. Salameh, A. Nothardt, E. Balthes, W. Schmidt, D. Schweitzer, J. Strempfer, B. Hinrichsen, M. Jansen, and D. K. Maude, Phys. Rev. B **75**, 54509 (2007).

[36] H. O. Jeschke, private communication and presentation at *ISCOM* (2017).

[37] M. Pinterić, P. Lazić, A. Pustogow, T. Ivek, M. Kuvezdić, O. Milat, B. Gumhalter, M. Basletić, M. Culo, B. Korin-Hamzić, A. Löhle, R. Hübner, M. Sanz Alonso, T. Hiramatsu, Y. Yoshida, G. Saito, M. Dressel, and S. Tomić, Phys. Rev. B **94**, 161105 (2016).

[38] R. Beyer, A. Dengl, T. Peterseim, S. Wackerow, T. Ivek, A. V. Pronin, D. Schweitzer, and M. Dressel, Phys. Rev. B **93**, 195116 (2016).

[39] A. Löhle, E. Rose, S. Singh, R. Beyer, E. Tafra, I. R, E. I. Zhilyaeva, R. N. Lyubovskaya, and M. Dressel, J. Phys. Condens. Matter **29**, 55601 (2017).

[40] M. Pinterić, D. Rivas Góngora, Z. Rapljenović, T. Ivek, M. Culo, B. Korin-Hamzić, O. Milat, B. Gumhalter, P. Lazić, M. Sanz Alonso, W. Li, A. Pustogow, G. Gorgen Lesseux, M. Dressel, and S. Tomić, Crystals **8**, 190 (2018).

[41] M. Dressel, N. Drichko, J. Schlueter, and J. Merino, Phys. Rev. Lett. **90**, 167002 (2003).

[42] N. Drichko, M. Dressel, C. A. Kuntscher, A. Pashkin, A. Greco, J. Merino, and J. Schlueter, Phys. Rev. B **74**, 235121 (2006).

[43] T. Kawai and A. Kawamoto, Phys. Rev. B **78**, 165119 (2008).

[44] T. Hiejima, S. Yamada, M. Uruichi, and K. Yakushi, Physica B **405**, S153 (2010).

[45] K. Noda, Y. Ihara, and A. Kawamoto, Phys. Rev. B **87**, 085105 (2013); Y. Ihara, M. Jeong, H. Mayaffre, C. Berthier, M. Horvatić, H. Seki, and A. Kawamoto, *ibid.* **90**, 121106 (2014); A. Ohnuma, H. Taniguchi, Y. Takahashi, and A. Kawamoto, J. Phys. Chem. C **122**, 24321 (2018).

[46] S. Kaiser, *Interplay of Charge Order and Superconductivity*, Ph.D. thesis, Universität Stuttgart, Stuttgart (2010).

[47] M. Glied, S. Yasin, S. Kaiser, N. Drichko, M. Dressel, J. Wosnitza, J. Schlueter, and G. Gard, Synth. Met. **159**, 1043 (2009).

[48] I. Olejniczak, B. R. Jones, Z. Zhu, J. Dong, J. L. Musfeldt, J. A. Schlueter, E. Morales, U. Geiser, P. G. Nixon, R. W. Winter, and G. L. Gard, Chem. Mater. **11**, 3160 (1999); B. R. Jones, I. Olejniczak, J. Dong, J. M. Pigos, Z. T. Zhu, A. D. Garlach, J. L. Musfeldt, H.-J. Koo, M.-H. Whangbo, J. A. Schlueter, B. H. Ward, E. Morales, A. M. Kini, R. W. Winter, J. Mohtasham, and G. L. Gard, *ibid.* **12**, 2490 (2000).